



**HAL**  
open science

## Estimation of GNSS Signals' Nominal Distortions from Correlation and Chip Domain

Jean-Baptiste Pagot, Paul Thevenon, Olivier Julien, Yoan Gregoire, Francisco Amarillo-Fernandez, Denis Maillard

► **To cite this version:**

Jean-Baptiste Pagot, Paul Thevenon, Olivier Julien, Yoan Gregoire, Francisco Amarillo-Fernandez, et al.. Estimation of GNSS Signals' Nominal Distortions from Correlation and Chip Domain. ION ITM 2015, Proceedings of the 2015 International Technical Meeting of The Institute of Navigation, ION, Jan 2015, Dana Point, California, United States. hal-01120942

**HAL Id: hal-01120942**

**<https://enac.hal.science/hal-01120942>**

Submitted on 1 Oct 2015

**HAL** is a multi-disciplinary open access archive for the deposit and dissemination of scientific research documents, whether they are published or not. The documents may come from teaching and research institutions in France or abroad, or from public or private research centers.

L'archive ouverte pluridisciplinaire **HAL**, est destinée au dépôt et à la diffusion de documents scientifiques de niveau recherche, publiés ou non, émanant des établissements d'enseignement et de recherche français ou étrangers, des laboratoires publics ou privés.

# Estimation of GNSS Signals' Nominal Distortions from Correlation and Chip Domain

J.B. Pagot, P. Thevenon, O. Julien, *ENAC, France*

Yoan Gregoire, *CNES, France*

Francisco Amarillo Fernandez, *ESA, the Netherlands*

Denis Maillard, *CapGemini, France*

## BIOGRAPHIES

**Jean-Baptiste Pagot** is a PhD candidate in the Department of Signal Processing and Satellite-based Navigation at the ENAC (Ecole Nationale de l'Aviation Civile) in Toulouse, France. He received his master degree as an Electronics and Telecommunication engineer in 2013 from the ENAC. He is currently working on GNSS Signal Distortions.

**Dr. Paul Thevenon** graduated as electronic engineer from Ecole Centrale de Lille in 2004 and obtained in 2007 a research master at ISAE in space telecommunications. In 2010, he obtained a PhD degree in the signal processing laboratory of ENAC in Toulouse, France. From 2010 to 2013, he was employed by CNES, to supervise GNSS research activities. Since the July 2013, he is employed by ENAC as Assistant Professor. His current activities are GNSS signal processing, GNSS integrity monitoring and hybridization of GNSS with other sensors.

**Dr. Olivier Julien** is the head of the Signal Processing and Navigation (SIGNAV) research group of the TELECOM laboratory of ENAC, in Toulouse, France. He received his engineer degree in 2001 in digital communications from ENAC and his PhD in 2005 from the Department of Geomatics Engineering of the University of Calgary, Canada. His research interests are turned towards the use of satellite-based navigation systems for safe navigation.

**Francisco Amarillo-Fernández** received his Master's Degree in Telecommunication by the Polytechnic University of Madrid (UPM) Spain in 1997, and his Master's Degree in Surveying Engineering by the UPM in 1992. He has been working for the ESA Navigation Directorate since 2001 and has participated/led in numerous research activities in the GNSS field since 1997.

**Denis Maillard** received his engineer degree in Electronic and Computer Engineering from Institut National des Sciences Appliquées de Rennes in 2010. Since 2011 he works as a GNSS engineer in the EGNOS

team of Capgemini Bayonne. He is currently in charge of the activities linked to GNSS signal processing.

**Yoan Gregoire** is radionavigation and radiolocation engineer in the navigation/location signals and equipment department in CNES, the French Space Agency. His GNSS activities cover signal processing and performance evaluation of GNSS systems. He is in charge of the development of a GNSS Signal Observatory which goal is to study signal deformation and their impact on user accuracy.

## ABSTRACT

This paper analyses two ways to investigate nominal distortions of GNSS signals. Firstly, these perturbations can be observed from the correlation function point of view and secondly, from the CDO (Chip domain observable) which is a way to extract the shape of such distortions directly from the digitized signal samples using the code periodicity. This method is also known as the Vision Correlator (NovAtel). [1]

These two techniques are compared in terms of capacity to observe and characterize GNSS signal nominal deformations. The CDO has the advantage to process only one specific part of the signal whereas the correlation function observable is less affected by the noise and is directly linked with the pseudorange estimation. As a conclusion, this publication proposes a new way to perform the Signal Quality Monitoring based on the Chip Domain Observable.

## INTRODUCTION

Nowadays, GNSS is useful in many fields and tends to reach better and better performances in terms of accuracy, availability and integrity. Some users (based as well on absolute or differential mode) can however still be strongly affected by slight measurement errors. Even if they represent 'supposedly' negligible errors, these deformations can deteriorate accuracy and/or integrity performances, as for example in civil aviation.

One example that is often overlooked is the presence of nominal distortions on the GNSS signal transmitted by the

satellite payload. Indeed, even in a fault free configuration (also called nominal case), signals transmitted by GNSS satellites are stained by small distortions. These distortions are generated by the payload, coming from the signal generation unit and the antenna. They generally appear as distortions of the PRN chips. Previous works put forward a coarse idea of these distortions:

- oscillations after each chip transitions and
- delay (lead or lag) between rising and falling edges of PRN chips

This phenomenon impacts the receiver processing and can introduce unwanted errors at different levels of the signal processing. This kind of problem was already tackled by different laboratories: Stanford ([2], [3], [4]), DLR ([5]) and CNES ([11]). Nevertheless, some questions remain about the time variation of such distortions, the best mean to estimate it, or more generally about the consistence of actual results.

The aim of this paper is to compare two processing techniques (one based on the correlation function and the other on the Chip Domain observable) regarding the visualization and characterization of nominal distortions.

First, an overview of the CDO and correlation function observation techniques will be provided. Then, advantages and drawbacks of these two methods will be described. In particular, a theoretical study of the performance in term of noise impact of both observation techniques will be presented. Following an innovative derivation, a study of CDO performances will be proposed and this method will be utilized to visualize nominal distortions. Performances of the CDO are shown to be not as good as those of the correlation function in terms of observation noise, but some phenomena such as distortions on the chip transitions becomes more visible using the CDO. Finally, the work will be supported by results obtained from data collected by a CNES 2.4m high gain antenna (Toulouse, France) and a German Administration (Federal Network Agency for Electricity, Gas, Telecommunication, Post and Railway) 7m high gain antenna (Leeheim, Germany). Only GPS L1 C/A signals are considered. A thorough description of the experimental set-up and required processing will be exposed. The use of two data collection locations allows to have a better view of phenomenon that could be due to the local set up (receiving bandwidth, specific receiving hardware distortions, etc...) and thus to isolate nominal distortions really generated by the satellite payload. The last part of this article opens a discussion about a new way to monitor the signal: perform the Signal Quality Monitoring thanks to the Chip Domain Observable.

## PROPOSED TECHNIQUES TO INVESTIGATE NOMINAL DISTORTIONS

In this first part, both the Chip Domain Observation and the correlation function processing will be introduced

independently. A third technique based on the S-curve and thus on the correlation function processing will be described.

The characterization of nominal distortions can be difficult as it depends on many parameters: the receiver configuration has an impact on the resulting tracking error, the satellite type (for instance satellites from different GPS blocks, potentially using different technologies) can create different error magnitudes, the modeling of the distortion can be complex although simple models based on a limited number of parameters are generally used [2], etc. The modeling of such distortions is also challenging: currently oscillations present after each PRN chip transition are generally approximated by a second order filter even if it has been shown that it is not the case [6].

One way to estimate these distortions is to observe them directly at the signal level or to visualize their effect at different stages of the receiver processing (correlation function, S-curve, pseudo-range...). However, specific equipment and/or processing are required to observe these distortions: high-gain antennas [3], [5], [11] multi-correlator receivers [7], long integration time [11]...

### First technique: Chip Domain Observable

Nominal distortions are impacting the user due to their consequences at different level of the receiver processing. However, causes of these small perturbations find their origin on the disturbance of the temporal signal. Then the first approach is to directly estimate the chip distortion. The Chip Domain Observable (CDO) is a processing of the GNSS signal that permits to observe an average GNSS signal. This ‘observed part’ can be positive/negative chips, rising/falling chip transition, part of the entire code periods... This section will focus on chip transitions. An ‘average’ chip transition is obtained by superimposing every transition of a given type (e.g. rising edge) during a chosen time window called the “observation time”, in order to average out the noise affecting the temporal samples of the GNSS signal.

Taking back notation of [7] the CDO can be described by:

- $CDO_k$  is the  $k$ -th value of the averaged signal amplitude in a given delay bin
- $rt_k$  is the  $k$ -th instant relative to a transition type, expressed in fraction of chips. This delay corresponds to the center of the  $k$ -th delay bin.
- $\Delta_{bin}$  is the size of the bin in seconds. It corresponds to the time resolution with which the transition is observed. This delay is considered constant for all bins if bins are uniformly distributed.
- $N_{bin}$  is the number of delay bins on which the CDO is computed. We have the relation:  $\Delta_{bin} = T_c/N_{bins}$  where  $T_c$  is the chip period if the ‘observed part’ is one chip long and if bins

are uniformly distributed along this observed part.

Figure 1 gives an example illustrating parameters introduced. In this case, a rising transition is visualized with  $N_{bin} = 10$ .

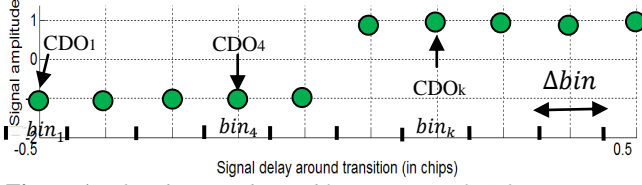


**Figure 1.** Chip domain observables (green circles) for a rising transition 10 bins

### Second technique: Correlation Function Observable

Another way to characterize nominal distortions is the study of their impact on the receiver processing [4]. Following classical schemes of signal processing in a GNSS receiver, the first workable observable is the correlator output and the last one is the pseudorange estimation. As a consequence, this paper will be focused on the analysis of the correlation function and the S-curve zero crossing.

The correlation output is equal to the convolution between the received signal (with its imperfections) and a non-distorted local replica. That is why the correlation function contains information about distortions affecting the satellite signal. These distortions can be seen as a filtering of an ideal signal. Mathematically, the following formula gives the link between the correlation function at the receiver  $R$  and transfer functions.

$$R(\tau - \tau_{est}) = FT^{-1}(H_t(f)H_r(f)DSP(f)e^{-2\pi f\tau_{est}})$$

With:

- $\tau_{est}$ : estimated delay between the received signal and the local replica
- $FT^{-1}$ : inverse Fourier transform
- $H_t(f)$ : transmission transfer function
- $H_r(f)$ : reception transfer function
- $DSP(f)$ : undistorted signal power spectral density

In the same way, we can define several parameters:

- $R_k$  is the  $k$ -th value of the correlation function amplitude at a given point of the function.  $k = 0$  at the correlation function top (the prompt output).
- $\tau_k$  is the value of the  $k$ -th correlation outputs delay.  $\tau_0 = 0$  (for the prompt output)
- $\Delta\tau_k$  is the distance along the time axis between two outputs of the correlation function, expressed in chip fraction. It corresponds to the resolution with which the correlation function is

observed. We consider in this document that the distribution of correlator outputs is uniform. And then for all  $k$ ,  $\Delta\tau_k = \tau_{k+1} - \tau_k = \Delta\tau$ .

- $N_{corr}$  is the number of correlator outputs where the correlation function is estimated. For simplicity, we consider that  $N_{corr}$  is an odd number. We have the relation:  $\Delta\tau = 2 \times T_c / (N_{corr} - 1)$  (here the correlation function is  $2 \times T_c$  large).
- $CS_k$  represents the correlator spacing of the  $k$ -th correlator pair.  $CS_k = \tau_k - \tau_{-k} = 2 \times k \times \Delta\tau$ .

An illustration is given in Figure 2 and 3, respectively showing parameters on an undistorted and a distorted correlation function with  $N_{corr} = 7$ . Circles represent correlator outputs, and blue color symbolizes the tracking correlator pair.  $\epsilon_{track,r}$  is the tracking error introduced by the reference correlator pair (here the tracking pair).

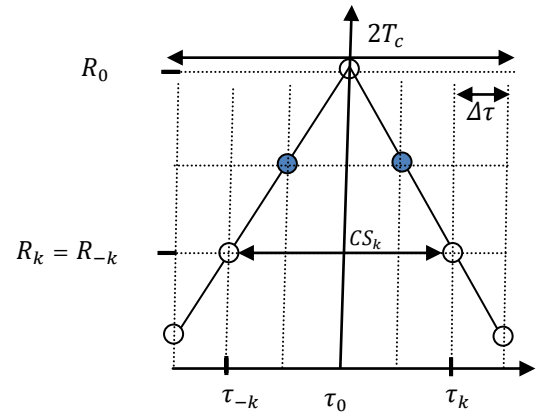


**Figure 2.** Correlation function parameters description for an undistorted signal

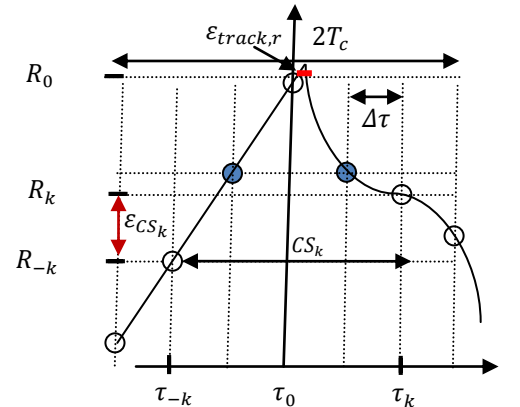


**Figure 3.** Correlation function parameters description for a distorted signal

It is noticeable that in the ideal case (undistorted correlation function),  $R_k = R_{-k}$  for all  $k$ .

However, in the general case a correlator pair is not necessarily defined by two symmetric correlator outputs. Then, the relation becomes:

$$\begin{cases} R_k - R_{-k} = 0 + n \\ \text{if outputs } k \text{ and } -k \text{ are used for the tracking} \\ R_k - R_{-k} = \varepsilon_{CS_k} + n \text{ otherwise} \end{cases}$$

With  $\varepsilon_{CS_k}$  the difference of correlator outputs ordinate between the  $k$ -th of correlator pair outputs and  $n$  is a Gaussian white noise affecting this difference of correlators outputs. For two close correlator outputs, this noise can be correlated.

### Third technique: S-curve zero crossing

In this document, only the Early minus Late discriminator will be developed.

The S-curve represents the discriminator output. As a consequence, a zero-crossing of the S-curve represents a point at which the tracking loop can be locked. In this sense, a zero-crossing of this S-curve represents the potential synchronization error once the tracking loop has converged. For code delay tracking the S-curve is function of the discriminator and thus correlator outputs' values for a given  $CS_k$ . The discriminator output can be expressed as  $R_k - R_{-k}$  (Early minus Late discriminator).

The goal of the tracking process is to reach a state where tracking pair  $r$  satisfies the relation:  $R_r - R_{-r} = 0 + n$ .

In this condition and in the ideal case, the configuration illustrated on the figure 2 is reached. For the tracking pair,  $\varepsilon_{CS_r} = 0$ , but this is also the case for all other correlator pairs ( $\varepsilon_{CS_k} = 0$ ).

As illustrated with a distorted correlation function, the tracking pair (in blue) satisfies  $R_r - R_{-r} = 0 + n$ , but the user is impacted by a tracking error  $\varepsilon_{track,r}$ . This tracking error is correlator spacing ( $CS_r$ ) dependent.

To simplify the problem, we will not study the absolute tracking error of a tracking pair, but the relative tracking error existing between a reference correlator pair and the  $k$ -th correlator pair ie.  $\varepsilon_{track,k} - \varepsilon_{track,r}$ .

## COMPARISON OF CDO AND CORRELATION FUNCTION APPROACH

The objective of this section is to compare the chip domain and the correlation function observation. Firstly, a short overview of each technique's advantages will be provided. Secondly, the comparison will be performed regarding their relative accuracy. To finish, a mathematical reasoning will be exposed in order to show the mathematical similitude between the two methods. The two first points put forward processing differences whereas the last point is focused on similarities.

### Advantages of each method

This discussion was already tackled in [8] with more details and is summarized here.

Advantages of the CDO are:

- Inputs of the CDO (IF signal samples) are given directly by the RF front-end while multi-correlator outputs have to be computed specifically for a given code delay.
- The noise affecting the CDO is uncorrelated white noise (or weakly correlated by the RF front-end filter), while the noise affecting a correlator outputs is correlated through the multiplication with the local replica.
- The resolution of the CDO can be increased beyond the sampling frequency of the signal thanks to a principle called dithered sampling. [9]
- The CDO permits to observe independently different types of signal observables. An important consequence is that falling and rising edges can be visualized separately whereas it is not possible on the correlation function.

However, correlation function observables have advantages compared to chip domain observables because of the place of the correlation operation in the tracking processing. Then:

- The tracking is directly dependent upon the correlation function. As a consequence, the distortions visible on the correlation function are directly related to the pseudorange errors. In this sense, the distortion of the correlation function appears more representative of the potential problems on the pseudoranges. A corollary of this is that some of the distortions visible on the CDO could be filtered/transformed by the correlation process which is based on the entire PRN code. Consequently some signal distortions could not influence the tracking process.
- Correlation processing is already available in nominal receivers, although multi-correlator outputs are not yet widely available.
- Correlator outputs are much less noisy than IF samples.

### Standard deviation consideration

The aim is now to quantify the standard deviation of the noise affecting the CDO ( $\sigma_{CDO}$ ) and correlator outputs ( $\sigma_{Corr}$ ). Considering that a noise with a standard deviation  $\sigma_n$  is affecting the incoming signal at the output of the RF front-end, the following relation can be written:

$$\sigma_X = \frac{\sigma_n}{\sqrt{N_X P_s}} \quad (1)$$

Where

- X indicates the processing technique: CDO or correlation.
- $N_X$  is the number of samples involved in the processing X and
- $P_s$  is the received GNSS signal power.

As it was shown in [7], in the CDO context, the expression of the average number of samples in one bin is:

$$N_{CDO} = F_s \Delta_{bin} \frac{T_{obs}}{T_{code}} N_{observed\_part\_code} \quad (2)$$

With

- $F_s$  the sampling frequency in Hz
- $T_{obs}$  the observation time in seconds
- $T_{code}$  the code period in seconds
- $N_{observed\_part\_code}$  the number of the wanted 'observed part' per code period.
- $\Delta_{bin}$  is the size of the bin in seconds

In the correlation function context, one correlator output is computed according to a number of signal samples equal to:

$$N_{Corr} = F_s T_{obs} \quad (3)$$

From equation (2) and (3), it can be noted that:

$$\frac{\sigma_{CDO}}{\sigma_{Corr}} = \sqrt{\frac{N_{Corr}}{N_{CDO}}} = \sqrt{\frac{T_{code}}{N_{observed\_part\_code} \Delta_{bin}}} \quad (4)$$

The equation (4) is a general equation. For the following we will consider a particular case. The study will be focused on the transitions observation. The 'observed part' is chosen with a  $T_c$  length and bins are uniformly distributed along this time interval. It entails that:

- $N_{observed\_part\_code} = N_{trans}$  with  $N_{trans} \approx 250$  the number of rising or falling transitions in one code period.
- $\Delta_{bin} = T_c / N_{bins}$  where  $N_{bins}$  is the number of bins in the 'observed part'.

In this particular case, equation (4) becomes:

$$\frac{\sigma_{CDO}}{\sigma_{Corr}} = \sqrt{\frac{N_{Corr}}{N_{CDO}}} = \sqrt{\frac{N_{bin} T_{code}}{N_{trans} T_c}} \approx \sqrt{4 \times N_{bin}} \quad (5)$$

Then, the computation of  $\sigma_x$  is possible considering that the noise is an averaged white Gaussian noise with a standard deviation [8]:

$$\sigma_n = \sqrt{P_n} = \sqrt{\frac{1}{2} \cdot P_s \cdot \frac{F_s}{C/N_0}} \quad (6)$$

Where  $C/N_0$  is the carrier to noise density ratio expressed in Hz (natural scale). The factor 1/2 comes from the fact that we are looking at the noise affecting only one component of the signal (in-phase and quadrature components). This value of signal power does not take into account possible filtering of the noise at the RF-front end.

Figures 4, 5 and 6 represent the processing outputs averaged over two seconds. They were obtained with a GPS signal generated by a simulator with  $C/N_0$  equal to 60 dB-Hz and a 7 MHz sampling frequency. In this condition, chips are perfect rectangles. Differences between an ideal noisy-free processing and a noisy observation are also presented in the inferior part of each figure. That gives an idea of the noise affecting the results. Figure 4 shows a result for the correlation function, 5 and 6 for the chip domain observable considering that one chip is divided in 1000 bins (respectively 100 bins). On the correlation function 4, this difference is affected by a correlated white noise. This noise correlation is due to the correlation process of the incoming noisy signal with the local replica.

Associated standard deviations were evaluated considering a 20 msec processing "observation time". The estimation is based on 100 measurements. We obtained:

- $\sigma_{corr} = 5,3 \cdot 10^{-3}$  (compared to theoretical case:  $\sigma_{corr} = 5,0 \cdot 10^{-3}$ ),
- $\sigma_{CDO} = 0,32$  considering 1000 bins (instead of 0,31) and
- $\sigma_{CDO} = 0,14$  considering 100 bins (instead of 0,10).

These simulation results confirm the validity of the formulas given by the equations (1), (2), (3) and (6).

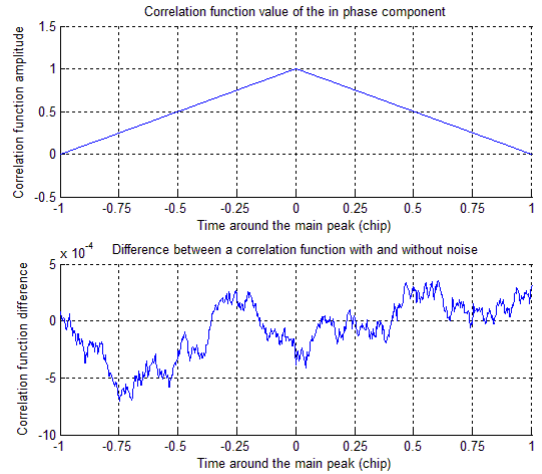


**Figure 4.** Correlation function observables (top), and associated difference with non noisy observables (bottom)

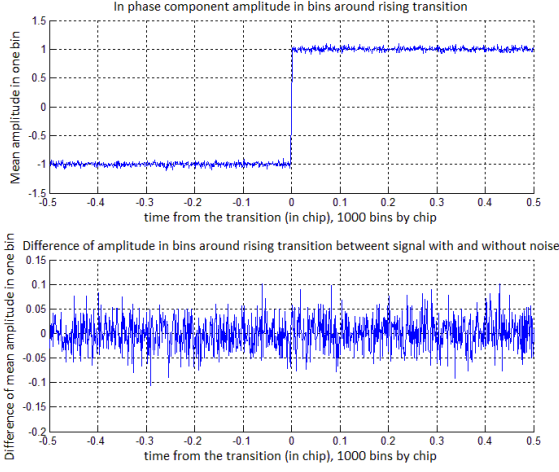


**Figure 5.** Chip Domain observables (top), and associated difference with non noisy observables (bottom), 1000 bins/chip

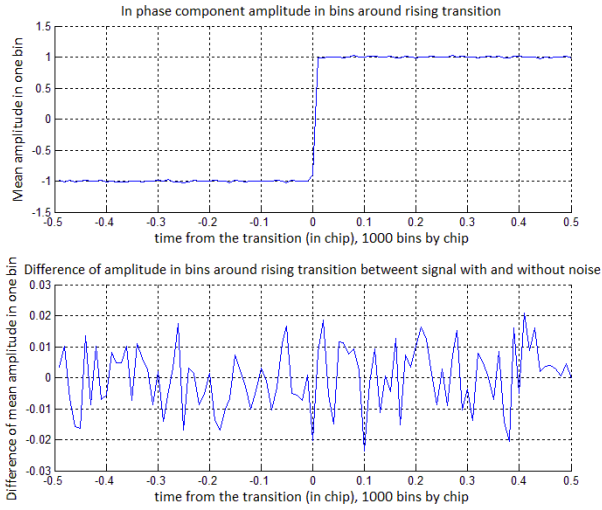


**Figure 6.** Chip Domain observables (top), and associated difference with non noisy observables (bottom), 100 bins/chip

### Mathematical consideration

This section aims at establishing the relation between the observation at the correlation and the chip levels. For that, on one hand, the true mathematical expression of the correlation function will be expressed and on the other hand, a CDO-related correlation function will be established. These two expressions will be compared.

#### Mathematical expression of the correlation function

Without Doppler offset and considering a sampled signal, the chip sequence expression would be:

$$c(t, f_{dop} = 0) = \sum_{p=-\infty}^{+\infty} \sum_{k_c=0}^{L-1} c_{k_c} \cdot \text{Rect}_{T_c}(t - k_c T_c - p L T_c) \quad (7)$$

where

- $T_c$  is the chip duration in seconds

- $L$  is the number of chips in the PRN code. For L1 C/A,  $L = 1023$ .
- $c_{k_c}$  is the value of the  $k$ -th chip of the PRN code.
- $\text{Rect}_{T_c}(t) = \begin{cases} 1 & \text{for } t \in [0, T_c] \\ 0 & \text{elsewhere} \end{cases}$  is the rectangle function corresponding to the BPSK modulation with a chip rate of  $1/T_c$ .
- $k_c$  represents the chip index in the PRN code and  $p$  the code period index. For simplicity, the  $p$  indices will be removed. Consequently,  $k$  will be introduced and may takes value higher than  $L$ .  $k$  and  $k_c$  are linked by the relation:  $k_c = k \bmod(L)$ .

We are now considering discrete time ( $t_i$ ) because the signal is digitized. Moreover, in the receiver, taking into account a slice of the sampled signal with duration  $T_{obs}$ , the expression of the chip sequence becomes:

$$c(t_i, f_{dop} = 0) = \sum_{k=0}^{T_{obs}/T_c} c_k \cdot \text{Rect}_{T_c}(t_i - k T_c) \quad (8)$$

Then the autocorrelation function of this slice of signal is defined by:

$$\begin{aligned} R(\tau_j) &= (c * c)(\tau_j) = \sum_{i=0}^{T_{obs}/T_c} c(t_i) c(\tau_j - t_i) \\ &= \sum_{i=0}^{T_{obs}/T_c} \left( \sum_{k=0}^{T_{obs}/T_c} c_k \cdot \text{Rect}_{T_c}(t_i - k T_c) \sum_{k'=0}^{T_{obs}/T_c} c_{k'} \cdot \text{Rect}_{T_c}(\tau_j - (t_i - k T_c)) \right) \end{aligned}$$

Moreover for all  $k \neq k'$ , the correlation value doesn't correspond to a correlation peak value:

$$\begin{aligned} &c_k \cdot \left( \text{Rect}_{T_c}(t_i - k T_c - p L T_c) \right) \\ &\cdot c_{k'} \cdot \left( \text{Rect}_{T_c}(\tau_j - (t_i - k' T_c - p L T_c)) \right) \approx 0 \\ &\text{for } \tau_j \in [-T_c, T_c] \end{aligned} \quad (9)$$

It entails that:

$$\begin{aligned} R(\tau_j) &= \sum_{i=0}^{T_{obs}/T_c} \sum_{k=0}^{T_{obs}/T_c} \left( c_k \cdot \left( \text{Rect}_{T_c}(t_i - k T_c) \right) \right) \\ &\left( c_k \cdot \text{Rect}_{T_c}(\tau_j - (t_i - k T_c)) \right) \\ &\text{for } \tau_j \in [-T_c, T_c] \end{aligned}$$

Then, thanks to periodicity properties, it is possible to reduce the problem to one chip:

$$R(\tau_j) = N_{Corr} \sum_{i=0}^{T_c/T_s} \left( \text{Rect}_{T_c}(m_i) \right) \left( \text{Rect}_{T_c}(\tau_j - (m_i)) \right)$$

*for*  $\tau_j \in [-T_c, T_c]$  and  $m_i = t_i \bmod T_c$  (10)

This last expression corresponds to the mathematical form of the correlation process and leads to the well-known triangular shape of the correlation function. We recognize that the number of samples involved in the correlation process is equal to  $N_{Corr}$ .

Mathematical expression of the correlation function obtained from the CDO assuming the chips are well represented by the CDO.

The CDO mathematical expression can be written as the series of samples in each bin. In this part, only positive chip are considered and the observed part is  $T_c$  long. Each signal samples have a time stamp  $t_i$  Doppler corrected.

Then, in the bin  $k$  we have *for*  $m_i \in \left[ rt_k - \frac{\Delta bin}{2}, rt_k + \frac{\Delta bin}{2} \right]$  ( $m_i = t_i \bmod T_c$ ):

$$\begin{aligned} CDO_k &= \sum_{k_1=0}^{N_{observed\ part}} (c(m_i - k_1 T_c)) \\ &= \sum_{k_1=0}^{N_{observed\ part}} \left( 1 \cdot (\text{mean\_Rect}_{T_c}(rt_k)) \right) \\ &= N_{observed\ part} * \text{mean\_Rect}_{T_c}(rt_k) \end{aligned}$$

Where

- $k_1$  is the index of the studied transition (e.g. rising transition)
- $N_{observed\ part} = \frac{T_{obs}}{T_{code}} N_{observed\ part\_code}$
- $\text{mean\_Rect}_{T_c}(rt_k)$  is the mean value of samples with a time stamp  $m_i \in \left[ rt_k - \frac{\Delta bin}{2}, rt_k + \frac{\Delta bin}{2} \right]$ .

This mean is computed from  $\frac{\Delta bin}{T_s}$  samples. Then, we recover the number of samples involved in the CDO computation:  $N_{CDO}$  from equation (2).

Chip domain observables can be convoluted with a perfect rectangular shape in order to obtain a correlation function from the CDO.

Now,  $\tau_k$  is used instead of  $\tau_j$  to show that the sampling frequency and the CDO bin number are independent.

Making the convolution of  $CDO_k$  with a chip representing the local replica waveform (a rectangular function of length  $T_c$  for GPS L1 C/A) leads to:

$$R_{CDO}(\tau_k) = CDO * \text{Rect}_{T_c}(\tau_k) \quad (11)$$

$$\begin{aligned} &= \sum_{k=0}^{N_{bin}} (CDO_k) \left( \text{Rect}_{T_c}(\tau_k - (rt_k)) \right) \\ &= N_{observed\ part} \sum_{k=0}^{N_{bin}} \left( \text{mean\_Rect}_{T_c}(rt_k) \right) \left( \text{Rect}_{T_c}(\tau_k - (rt_k)) \right) \end{aligned}$$

## Conclusion

With the aforementioned assumption, and as expected, it appears that the correlation and the chip observable convoluted by a rectangular shape have the expression (with the approximation involved by the equation (9)). Thus, the CDO and the correlation processing are mathematically close. If all chips are assumed and if only one bin is considered, the mathematical expression of the  $R_{CDO}(\tau_k)$  is equal to  $R(\tau_k)$ .

In this part, a comparison between the correlation and the chip domain processing was tackled. Among these differences, it was shown that the CDO has the advantages to visualize a precise portion of the signal (chip, transition, entire code...). However, this benefit is balanced by the fact that the standard deviation of the noise affecting the CDO is higher by a factor  $\sqrt{4 \times N_{bin}}$ . Finally, mathematical derivations indicate that the correlation process and the convolution of the CDO with an ideal rectangle lead to the same results to a factor  $4 \times N_{bin}$ .

To conclude, it is important to underline the advantage of focusing only on one part of the signal. For example it is possible to see independently distortions due to a rising transition. On the contrary, the correlation function firstly combines deformation of rising and falling transitions which could be different. Secondly, the correlation process is an average of the entire signal. Thus, it takes into account chip weekly deformed because not behind a transition. This last point could entail a mitigation of nominal deformation on the correlation function. This brings advantages for pseudo range estimation but the CDO seems more suitable for signal monitoring. The last part of this paper will illustrate this concept.

## DATA COLLECTION

In the following, results from real signals will be presented and interpreted.

A high gain antenna is useful in order to obtain a sufficiently good signal observation. Indeed, after travelling the distance separating the satellite and an antenna located on Earth, the GNSS signals are below the noise floor of usual measurement devices. It is therefore advantageous to amplify the received signal in order to better observe it. In our case, this was performed thanks

to two directive antennas with the following features described in the table 1.

The collected signal was then digitized by a dedicated signal digitizer, called BitGrabber2 and developed by CNES [10] with a sample frequency of 125 MHz, a 8-bit quantization and a 3dB bandwidth of 70 MHz.

Antenna holder	German administration	CNES
Antenna site	Leeheim (Germany)	Toulouse (France)
Antenna diameter	7 m	2.4 m
Antenna bandwidth	1000 – 2000 MHz	1100 – 1650 MHz
Collection period	Mars 2012	May-July 2014

Table 1. Antenna and data characteristics

Thanks to the antenna directivity, it can be considered that multipath are not perturbing our signals. The received  $C/N_0$  is around 70 dB/Hz and 80 dB/Hz Annex 1 shows a description of all available PRNs for this study.

## NOMINAL DISTORTIONS USING THE CORRELATION PROCESS

In this part, two methodologies will be used in order to visualize nominal distortions on real signals from the correlation process:

- Directly on the correlation function.
- Using the S-curve zero crossing observable.

### Correlation function observable

The first technique, most natural, to characterize nominal distortions is the computation of the correlation function. The purpose is to correlate the received signal with a local replica over a long duration (including non-coherent summations) in order to reduce the standard deviation of the noise affecting the observable [11]. Figure 7 shows the difference between an ideal correlation function and the one affected by nominal distortions. The ideal correlation function is a triangular function normalized by the slope of the nominal distorted correlation function. It is noticeable that these distortions cannot be considered or even approached by second order oscillations contrary to results established in the chip domain. [6]

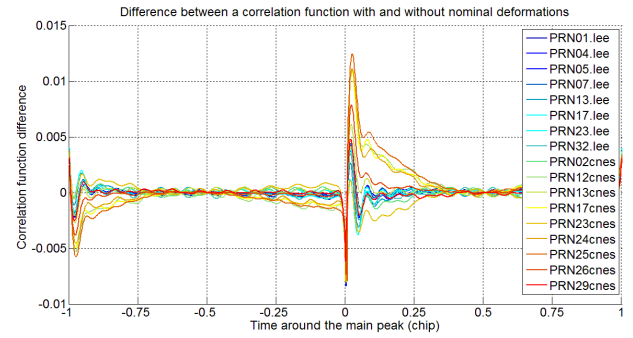


Figure 7. Difference between correlation functions with nominal distortions and a theoretical infinite bandwidth correlation function

This kind of plot cannot be used directly to estimate tracking biases affecting a user. Indeed, depending on the normalization of the ideal correlation function involved in the computation of the visualization of the correlation distortion difference, the plot will change. Here, the normalization is realized at -0.5 and 0.5 chip and no filtering is applied on the ideal function. Therefore, figure 7 only gives an idea of the deformation pattern. These results match with CNES study performed in 2012 [11].

### S-curve zero crossing

S-curves were obtained from an E-L discriminator. The analysis of the S-curve zero crossing function of the correlator spacing is a second approach to visualize the correlation distortion from a measurement point of view. Indeed, assuming that the code delay tracking loop has time to converge, the zero crossing of the S-curve translates directly into a pseudo-range bias. As introduced in the first section, on the x-axis, the tracking error regarding a correlator spacing  $CS_k$  is given.

In the present case, this tracking is expressed relatively to a reference tracking error ( $\varepsilon_{track,k} - \varepsilon_{track,r}$ ). This makes sense as it is difficult to assess the tracking bias due to the signal distortion directly (the actual tracking bias is also affected by other RF front-end characteristics). This computed differential tracking bias is directly convertible in a differential pseudorange error by multiplying it by the speed of light. The EGNOS and WAAS reference receiver characteristics are close. In particular, these reference receivers use an Early-Late spacing of 0.1 chip. In this publication this correlator spacing is used.

Figure 8 shows the differential tracking bias generated by nominal distortions for each correlator spacing between 0 and  $1,2T_c$  with respect to the reference tracking configuration for the data collected in Leeheim and at CNES. These results can be compared to Stanford University study presented in [4] with a few difference. Indeed the technique introduced in the section “satellite dish data processing method” of [4] is slightly different from this one. Here we compute the differential tracking error of a correlator pair considering  $R_k - R_{-k} = 0$  for each  $k$ . In the Stanford University study the differential tracking error is deduced from the value of  $R_k - R_{-k} =$

$\epsilon_{CS_k}$  and only the reference tracking pair satisfies  $R_k - R_{-k} = 0$ .

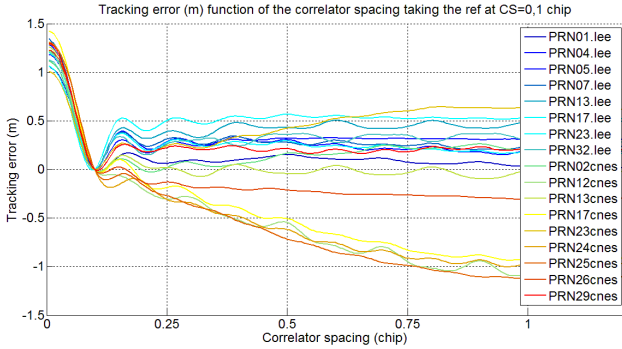


**Figure 8.** Tracking error function of the correlator spacing for different PRN.(reference at CS=0.1chip)

Results obtained by Stanford are presented in the Figure 9

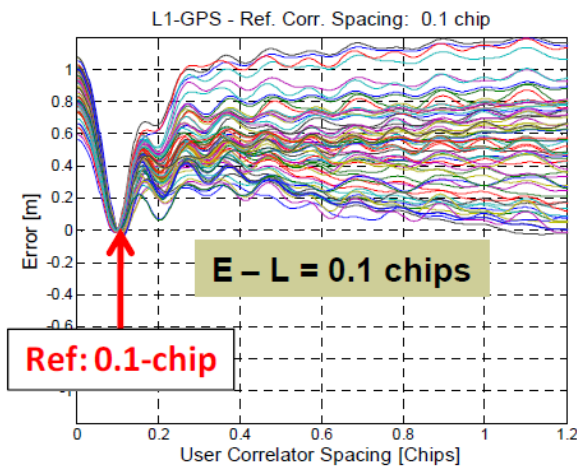


**Figure 9.** Tracking error function of the correlator spacing for different PRN from Stanford [4]

Looking at the results from Leeheim data, the Figure 8 complies with differential tracking bias plots that have been published in [11]. However, important negative slopes can be observed on these plots for some CNES data. A deeper comparison of results obtained from both antennas will be introduced in the next section.

Differences are noticeable regarding some CNES data with opposite curvature (deviation of the tracking error toward negative values rather than positive values). Nevertheless Leeheim data lead to similar shape of differential tracking bias curve than the Stanford study. It is noticeable, that differential tracking bias reported by Stanford are going from 0m to 1.2m compared to values from 0m up to 0.5m obtained with Leeheim data.

It seems that difference between results from the CNES and the DLR data set finds its origin before the analog to digital convertor because the signal digitizer and processing software were identical for both data sets. Thus, it is possible that the directive antenna used by CNES is the reason for these differences. Stanford picked up this problem in [4] and shown that time varying drifts were present in large dish measurements.

## CHIP DOMAIN NOMINAL DISTORTIONS

As already discussed, another technique to observe nominal distortions is to exploit directly the chip shape. Figure 10 shows the averaged rising transition for several PRN. These plots were obtained thanks to a 4-sec observation time. One noteworthy remark is that distortions are not exactly similar in the chip and in the correlation domain.

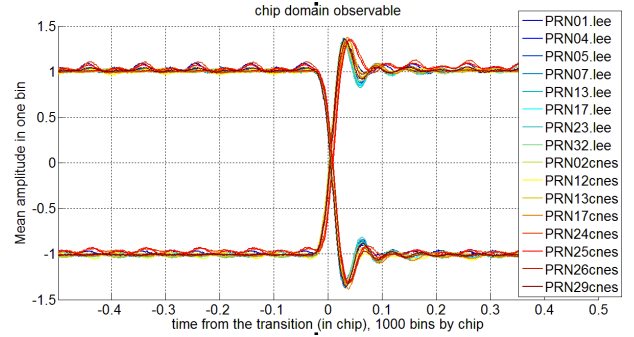


**Figure 10.** Chip domain observable of a rising transition, 1000 bins/chip

Nominal distortions are generally classified into analog (ringing phenomenon) and digital distortions (delay between rising and falling transitions). Until now in this document, these types of distortions were not separated, but just looked at jointly. To characterize these types of nominal distortions a way is to estimate deformation parameters. Analog parameters seem difficult to estimate because no models are perfectly representing the observed ringing effects.

On the other hand, the digital parameter is easier to evaluate, and this is one of the advantage of the chip domain observable. This parameter corresponds to the difference existing between the zero crossing of rising and falling transitions. Figure 11 is a zoom on transitions for the satellite 34 (Block II-A, PRN 4). It is noticeable that the two curves are not crossing the zero value at the same delay. Indeed, a lag of 1.50 bin exists on the falling edge compared to the rising one. Based on the selected size of the bin, this delay translates into a 1.5nsec delay. This result is consistent with Stanford University results [3].

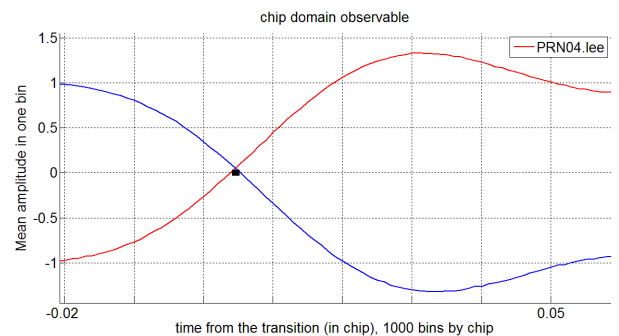


**Figure 11.** Zoom in the chip domain on zero crossing of rising and falling transition observables

The estimation of this delay was realized on other satellites and compared with Stanford University's outcomes.

Figure 12 shows that obtained delays are consistent with Stanford University results. These similarities are observed with CNES and Leeheim Data. Then, it shows that nominal distortions are relatively constant in time and that this error seems to be not introduced by the antenna. It could confirm that the satellite is the origin of such a deformation.

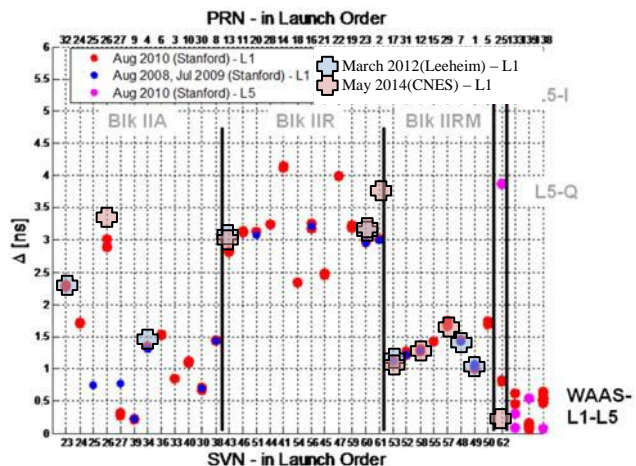


**Figure 12.** Superposition of Stanford results [3] with results obtained by another set of collected data. Visualization of the delay between rising and falling transitions.

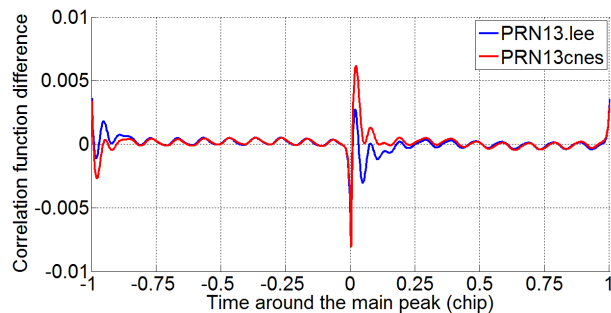
## INVESTIGATION OF THE NOMINAL DEFORMATION OBSERVED FROM TWO DIFFERENT ANTENNAS

In this section, only one PRN will be studied: the PRN 13. Differences between the two analyzed signals are:

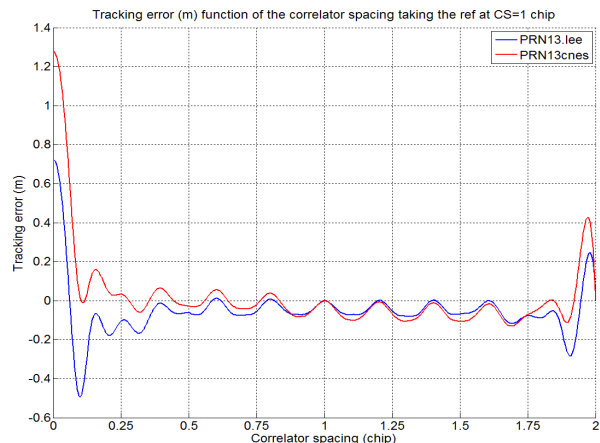
- Antennas: one 7m dish antenna from Leeheim (Germany), and the other one 2.4m antenna from CNES (France).
- Time of the transmission: one was captured in March 2012 (Leeheim) and the other in May 2014 (CNES).

Thus, it will be possible to establish nominal distortion changes due to time variation or/and antenna type.

Figure 13 and 14 put forward the comparison at the correlation function level.



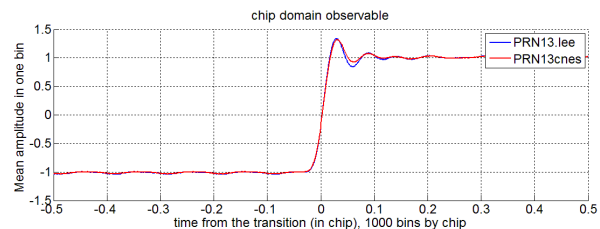
**Figure 13.** Comparison of nominal deformation for the same PRN making the difference of correlation functions with and without nominal distortions.



**Figure 14.** Comparison of differential tracking bias entailed by nominal deformation for the same PRN. (reference at  $CS=1$  chip)

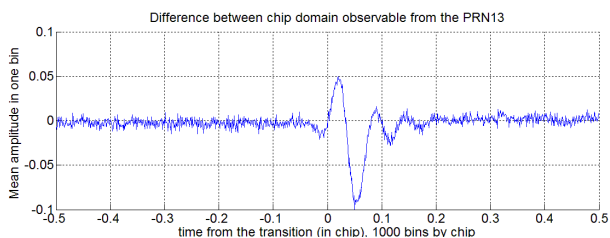
It is interesting to notice that nominal deformation ringing effects look very similar for both scenarios (especially from the figure 13). However, from the figure 14 it appears that general curvature of the two differential tracking bias plots is slightly different.

Figure 15 illustrates the impact of nominal distortions for chip domain observables.



**Figure 15.** Chip domain comparison of nominal deformation for the same PRN.

In order to visualize differences between these two curves, figure 16 represents the difference between them.



**Figure 16.** Difference between chip domain observable obtained from the same PRN.

The only remarkable difference appears at the transition level. This variation could be the signature of a filtering phenomenon. The origin of such filtering can come from the satellite filter but more probably from the receiver antenna.

## OPTIMAL OBSERVABLE REGARDING SIGNAL MONITORING

Advantages and drawbacks of CDO and correlation function observations were earlier presented in this article. The aim of this section is to find the observable the most affected by nominal perturbations in terms of amplitude distortions. These results should be particularly interesting regarding Signal Quality Monitoring. Indeed, if one domain is more sensitive to signal perturbations than the other, it could be attractive to monitor the signal in this domain.

In the second section of this paper, it was shown that the correlation function  $R$  and correlation functions obtained from the chip domain observable,  $R_{CDO}$ , are mathematically similar. The only differences are that  $R_{CDO}$  are more affected by the noise but with the advantage to be able to estimate specific sections of the signal (for example the rising transitions).

Figure 17 shows differences between three correlation functions established from the chip domain ( $R_{CDO}$ ) and the correlation function ( $R$ ). All functions are affected by nominal distortions. Three satellites with different payload technologies (ie from different GPS blocks) are considered. They are representative of the general behavior of each satellite block. Beforehand, correlation functions were normalized to 1 and then the associated theoretical infinite bandwidth correlation functions were subtracted. (The same method was applied in the section ‘correlation function observable’). The blue curve is based on computing the correlation function using the rising transitions only ( $R_{CDO,r}$ ), the green curve is based on the falling transitions only ( $R_{CDO,f}$ ), the red one on all transitions ( $R_{CDO,rf}$ ) and the black one is established from the classical correlation function.

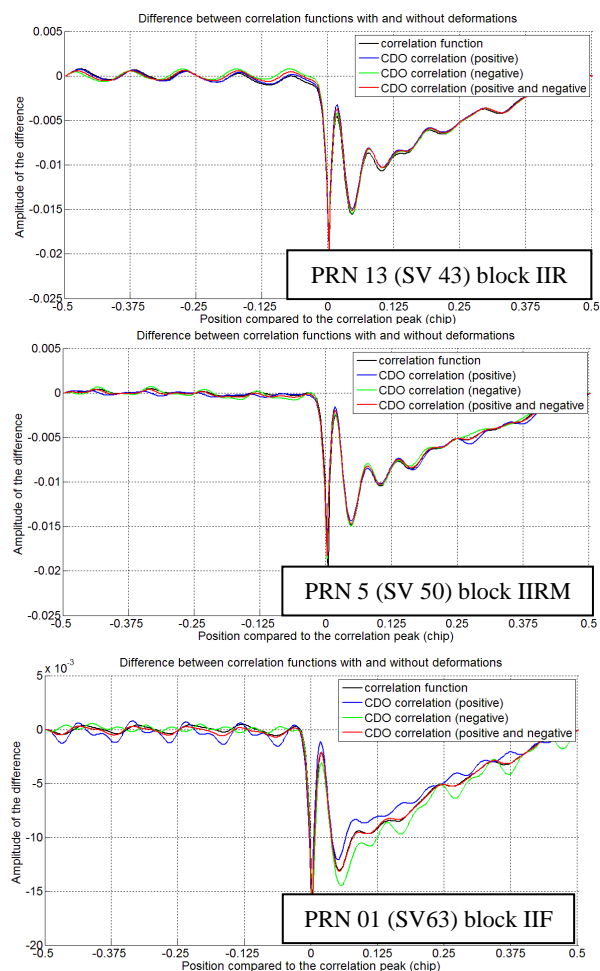


**Figure 17.** Difference between correlation function with nominal deformation and a theoretical infinite bandwidth correlation function for a block IIR (top), a block IIRM (middle) and a block IIF (bottom) satellite.

The correlation function  $R$  takes into account all chips (with or without transitions) and the correlation function  $R_{CDO,rf}$  is computed from all transitions. That is why the red and the black curves ( $R_{CDO,rf}$  and  $R$ ) are almost superimposed. However, the blue and the green curves ( $R_{CDO,f}$  and  $R_{CDO,r}$ ) are based only on one kind of transition and it explains the difference in shapes.

These illustrations (Figure 17) lead to two important conclusions:

- Nominal deformations are (slightly) dependent of the satellite payload technology. This particularity is enhanced by the chip domain observation. Indeed, blue and green plots have different behaviours according to distinctive blocks. It put forward the dissymmetry which could exist between positive and negative chips. If a deformation is affected rising and falling transition in the same way, blue and green curves should be identical. It seems that this symmetry exist for the IIR payload generation whereas it is less visible for IIRM block and especially for IIF satellites.

- A deformation affecting differently positive and negative chips is more visible on the chip domain than on the correlation function domain.

The first conclusion involves that nominal deformations are more perfectly characterized thanks to the chip domain. The remaining problem is that this observable is not directly linked to the user tracking error.

The second conclusion is that another method to perform Signal Quality Monitoring could be to focus on  $R_{CDO,f}$  and  $R_{CDO,r}$  and not  $R$  anymore. In this condition, the tracking and SQM would be computed from distinctive ways.

## CONCLUSION AND FUTURE WORKS

After introducing basic notions of correlation function and chip domain observable, a comparative study between these two methods was realized. Among advantages of the chip domain observation, a particularly attractive fact is that the observation can be focused on a particular part of the signal (chip, transition...) whereas the correlation function contained information about the entire signal. However, this advantage is compensated by the increase of the observation noise standard deviation in the chip domain. To conclude this comparative study, it was shown that the correlation function is mathematically similar to the convolution of a chip observable with an ideal rectangle. The only difference is that the correlation function is computed from all chips (positive and negative) and is consequently based on more samples.

Then, simulations on real signals were presented proposing several techniques to visualize nominal distortions. The S-curve zero crossing is especially interesting because it gives directly the tracking error that could affect users with different correlator spacing. Nonetheless, the observation of transition in the chip domain allows estimating easily digital signal distortions (delay between rising and falling transitions). The general idea is that correlation function and chip domain observables are complementary to fully characterize nominal distortions.

Afterwards, in order to assess nominal distortions time fluctuations, a focus was realized on one PRN. Indeed, the same signal was collected at two different epochs with two different antennas. It seems that tracking error entailed by nominal distortions is relatively constant. A slight difference appears at the chip transition and it seems that this effect could be brought by the antenna. More tests have to be done in order to understand the impact of the antenna or others components on observed differences. By this way, true nominal deformations (generated at the payload level) could be dissociated from other deformations considering here as nominal.

In the last part, it was beheld that distortions affecting differently a part of the signal (for example positive and

negative chip) could be more easily monitored from the chip domain observable than directly from the correlation function. Consequently, the Signal Quality Monitoring could be made in the chip domain and not on the correlation function anymore depending on the standard deviation affecting the observable. Future works will be to apply this technique to non nominal deformations in order to validate or not this way to complete the SQM.

This study was performed on GPS L1 C/A but future investigations have to be realized for GPS L5 and Galileo signals. Recently, the DLR has presented results about equivalent filters associated with nominal deformations and their impact on the differential bias [5]. An additional study could support these results being more focused on such distortion characterization. On the other hand, Stanford University has tackled the dual frequency (L1/L5) question in [12].

## REFERENCES

- [1] P. C. Fenton and J. Jones, "The theory and performance of NovAtel Inc.'s Vision Correlator," in *Proceedings of the 18th International Technical Meeting of the Satellite Division of The Institute of Navigation (ION GNSS '05)*, pp. 2178–2186, Long Beach, Calif, USA, September 2005.
- [2] Phelts, R.E., Walter, T., Enge, P., "Characterizing Nominal Analog Signal Deformation on GNSS Signals," *Proceedings of the 22nd International Technical Meeting of The Satellite Division of the Institute of Navigation (ION GNSS 2009)*, Savannah, GA, September 2009, pp. 1343-1350.
- [3] Wong, G., Phelts, R.E., Walter, T., Enge, P., "Characterization of Signal Deformations for GPS and WAAS Satellites," *Proceedings of the 23rd International Technical Meeting of The Satellite Division of the Institute of Navigation (ION GNSS 2010)*, Portland, OR, September 2010, pp. 3143-3151.
- [4] Wong, G., Phelts, R.E., Walter, T., Enge, P., "Alternative Characterization of Analog Signal Deformation for GNSS-GPS Satellites," *Proceedings of the 2011 International Technical Meeting of The Institute of Navigation*, San Diego, CA, January 2011, pp. 497-507.
- [5] S. Thaelert, et al, "Characterization of Nominal Signal Distortions and Impact on Receiver Performance for GPS (IIF) L5 and Galileo (IOV) E1 /E5a Signals", *Proc. ION GNSS 2014*, Tampa, FL, USA, Sep. 2014.
- [6] Mitelman, A.M. - SQM for GPS augmentation systems – PhD 2004
- [7] Phelts, E. - Multi-correlator Techniques for robust Mitigation of Threats to GPS Signal Quality – PhD 2001
- [8] P. Thevenon - Processing Technique and Performance of the Observation of EWF in the Chip Domain 2014
- [9] M. Pini, D.M. Akos, Exploiting GNSS Signal Structure to Enhance Observability, *Aerospace and Electronic Systems, IEEE Transactions on (Volume: 43,*

Issue: 4 ), Page(s): 1553 – 1566, Date of Publication : October 2007

[10] Ries, L., Perello Gisbert, J.V, ‘Bitgrabber 2, Operating Manual’, CNES and ESA project, October 2006.

[11] Lestarquit, L., Gregoire, Y., & Thevenon, P. (2012, April). Characterizing the GNSS correlation function using a high gain antenna and long coherent integration— Application to signal quality monitoring. In *Position Location and Navigation Symposium (PLANS), 2012 IEEE/ION* (pp. 877-885). IEEE.

[12] Wong, G., Chen, Y-H, Phelts, R.E., Walter, T., Enge, P., ” Mitigation of Nominal Signal Deformations on Dual-Frequency WAAS Position Errors “, *Proc. ION GNSS 2014*, Tampa, FL, USA, Sep. 2014.

32	GPS BIIA	Leeheim	14/03/2012 8:38
----	----------	---------	--------------------

**Annex 1: Available data description, GPS L1 C/A signals**

PRN	block	antenna	Start of data collection precise time (date: <i>dd/mm/yy</i> and hour: <i>hour:min</i> )
1	GPS BIIF	Leeheim	14/03/2012 8:34
2	GPS BIIR	Toulouse	13/05/2014 9:17
4	GPS BIIA	Leeheim	14/03/2012 11:14
5	GPS BIIRM	Leeheim	13/03/2012 15:31
7	GPS BIIRM	Leeheim	13/03/2012 15:15
12	GPS BIIRM	Toulouse	16/07/2014 11:26
13	GPS BIIR	Leeheim	14/03/2012 14:11
13	GPS BIIR	Toulouse	18/04/2014 9:57
17	GPS BIIRM	Leeheim	14/03/2012 9:54
17	GPS BIIRM	Toulouse	16/07/2014 11:02
23	GPS BIIR	Leeheim	14/03/2012 10:13
23	GPS BIIR	Toulouse	13/05/2014 8:40
24	GPS BIIF	Toulouse	18/07/2014 11:14
25	GPS BIIF	Toulouse	18/07/2014 11:19
26	GPS BIIA	Toulouse	13/05/2014 11:33
29	GPS BIIRM	Toulouse	17/07/2014 17:15